

OPEN
ANALYSIS

Semantic integration of diverse data in materials science: Assessing Orowan strengthening

Bernd Bayerlein¹✉, Markus Schilling¹, Philipp von Hartrott² & Jörg Waitelonis³

This study applies Semantic Web technologies to advance Materials Science and Engineering (MSE) through the integration of diverse datasets. Focusing on a 2000 series age-hardenable aluminum alloy, we correlate mechanical and microstructural properties derived from tensile tests and dark-field transmission electron microscopy across varied aging times. An expandable knowledge graph, constructed using the Tensile Test and Precipitate Geometry Ontologies aligned with the PMD Core Ontology, facilitates this integration. This approach adheres to FAIR principles and enables sophisticated analysis via SPARQL queries, revealing correlations consistent with the Orowan mechanism. The study highlights the potential of semantic data integration in MSE, offering a new approach for data-centric research and enhanced analytical capabilities.

Introduction

In Materials Science and Engineering (MSE), material and process data are generated using a variety of different techniques. For instance, assessing a component's degradation behavior at elevated temperatures necessitates data from both microstructural and mechanical analyses. The datasets resulting from these varied investigative techniques significantly differ in structure and format, posing a challenge for coherent integration and analysis^{1,2}. Despite the increasing reliance on utilizing enhanced material and process data for progress³, much of this data remains in heterogeneous and unstructured formats⁴, leading to a fragmented and underutilized knowledge base, which is considered a loss of valuable resources^{5,6}.

A central goal of digitalization in MSE is thus to achieve interoperability of material and process data from diverse sources, aligning with the FAIR principles⁷. Systematic data integration is expected to unlock valuable insights due to the intrinsic information and knowledge embedded within these data. Semantic Web technologies, particularly the development and application of ontologies, offer an effective approach to meet this challenge^{8–11}. As defined by Gruber, an ontology is a “formal and explicit specification of a shared conceptualization”¹². Ontologies facilitate context establishment, clear definition of meanings, formulation of relationships and rules, and linkages between data entities^{13,14}. They are ideal for the semantic integration of heterogeneous data sources, enhancing their usability and accessibility for both human and machine processing^{13,15,16}.

Ontologies are categorized into abstract, high-level forms such as top-level ontologies and mid-level ontologies, and specialized application ontologies. Application ontologies extend the concepts of mid-level ontologies and top-level ontologies to suit specific applications, inheriting their structural systematics crucial for interoperability^{17,18}. Such an ontological construct enables the integration of data into a structured, semantic exchange format – the Resource Description Framework (RDF)^{19–21}. The more data integrated into this semantic network or knowledge graph, the greater the accumulation of knowledge, enhancing the potential for artificial intelligence applications. For instance, improving natural language processing interpretability through ontological representations²², and increasing large language models accuracy²³. Knowledge representation also provides a descriptive basis for pattern recognition²⁴ and valuable information for decision making in areas such as machine learning and robotics^{15,25,26}.

¹Bundesanstalt für Materialforschung- und prüfung (BAM), Unter den Eichen 87, Berlin, 12205, Germany.

²Fraunhofer Institute for Mechanics of Materials IWM, Wöhlerstrasse 11, Freiburg, 79108, Germany. ³Leibniz Institute for Information Infrastructure (FIZ Karlsruhe), Hermann-von-Helmholtz-Platz 1, Eggenstein-Leopoldshafen, 76344, Germany. ✉e-mail: bernd.bayerlein@bam.de

Despite the promising emerging applications and documented benefits in the literature²⁷, MSE lacks practical, comprehensible examples demonstrating the steps of semantic data integration towards machine-processable knowledge representation^{9,15}. Our work addresses this gap by developing a “good practice” Jupyter Notebook demonstrator for the MSE community. We employ the Orowan mechanism, a fundamental MSE theory that describes material strengthening through dislocations and precipitates²⁸, as our use case. This demonstrator serves as a practical example of applying Semantic Web technologies in MSE, showing the use of ontologies and illustrating how valuable insights can be gained from heterogeneous data sources.

Our demonstrator addresses the following focal points:

- Methodical aggregation and structuring of two distinct, publicly available datasets from mechanical (tensile testing) and microstructural (dark-field transmission electron microscopy (DF-TEM)) characterizations of radial compressor wheels aged over several intervals.
- Development of an ontological framework using the PMD Core Ontology (PMDco) as a unifying mid-level ontology²⁹.
- Seamless semantic integration of both datasets using specific application ontologies for tensile testing and DF-TEM image analysis data.
- Creation of a queryable knowledge graph as a proof-of-concept for semantic interoperability.
- Conducting targeted information queries to generate new insights via digital workflows, followed by enriching the knowledge graph.
- Demonstrating the process of indirect knowledge generation by uncovering hidden patterns in datasets through the querying of correlatable value pairs leading to the derived Orowan’s law.

Results

In this section, we present the results of our research, which were obtained through information retrieval and analysis using the components of our Jupyter Notebook demonstrator, as referenced in³⁰. The methods employed for ontological data representation and semantic data integration, within an ontological framework focused on the PMDco, are presented in detail in Section [Ontological framework](#) and Section [Implementation of RDF graphs and ABox data instantiation](#).

By leveraging Semantic Web technologies, we establish meaningful links between two distinct datasets: the mechanical properties derived from tensile testing³¹ and the microstructural characteristics obtained from DF-TEM image analysis³² (see Section [Tensile testing](#) and [DF-TEM imaging](#), respectively). This integration is achieved by embedding these datasets into a unified knowledge graph, where mid-level concepts serve as bridges, enhancing both data interoperability and comparability. The incorporation of these datasets into a knowledge graph is essential for developing a robust framework, which leverages SPARQL Protocol and RDF Query Language (SPARQL) queries for information retrieval and knowledge discovery³³. Our approach enables exploration of the relationships between the mechanical and the microstructural properties of radial compressor wheels, offering deeper insights into their interdependence and aging behavior.

Data retrieval, processing, and knowledge graph integration. This section describes our approach for managing and analyzing the data instantiated in Section [Implementation of RDF graphs and ABox data instantiation](#), as well as for extending the knowledge graph with the newly derived results. The process involves three key steps: selective data retrieval using SPARQL queries (i), data processing through script-based workflows (ii), and integrating data outcomes back into the existing knowledge graph (iii), thereby enhancing it.

- Initially, we extract specific information from the RDF dataset using precisely formulated SPARQL query that addresses the local triple store. For instance, Box 1 illustrates a designed query for processing microstructural data, retrieving details such as specimen images, material states, X and Y coordinates, and radii of precipitates from the DF-TEM image-based analysis dataset. The dataset relies on a conventional image processing procedure for analyzing precipitates, which includes several steps such as initially applying edge-preserving median filtering to the DF-TEM raw images, followed by manual thresholding for precipitate segmentation, as elaborated in Section [DF-TEM imaging](#) and referenced in³⁴. Once this information is retrieved, the data is structured and prepared for further analysis, exemplifying the use of our locally managed RDF environment in drawing relevant insights from the data.
- Next, the retrieved data is processed using a script-based workflow. Our primary focus is on determining the mean distances between precipitates and understanding how these mean distances vary across different material states, especially due to aging. For this purpose, we employ the Delaunay triangulation method³⁵ to calculate precipitate distances for each material state and corresponding sets of images (see Table 1 for details). Each image’s precipitates are plotted using their X and Y coordinates. We use Delaunay triangulation to form triangles with precipitates as vertices, calculating the Euclidean distances between these vertices (Figure 1(a)). The resulting precipitate distances are then depicted in a cumulative distribution function plot (Figure 1(b)).
- The calculated average precipitate distances, obtained by determining the mean values, are integrated into the existing knowledge graph. This involves creating a new class within the Precipitate Geometry Ontology (PGO), named `pgo:AveragePrecipitateDistance`, as a subclass of `pgo:PrecipitateDistance`. The computed data for the material states are then instantiated as instances of this new class, thereby enriching and expanding the knowledge graph.

Material State	Aging Temperature	Aging Time	Specimens	Images
T61	—	—	2	12
190°C_250h	190°C	250 h	1	11
190°C_1000h	190°C	1,000 h	1	12
190°C_2500h	190°C	2,500 h	2	17
190°C_5000h	190°C	5,000 h	2	23
190°C_8760h	190°C	8,760 h	2	19
190°C_25000h	190°C	25,000 h	2	21

Table 1. Summary of DF-TEM image analysis dataset employed in this study.

```

PREFIX pmdco: <https://w3id.org/pmd/co/>
PREFIX pgo: <https://w3id.org/pmd/pgo/>
PREFIX qudt: <http://qudt.org/vocab/unit/>

SELECT DISTINCT ?tem_proc \
?specimen \
?specimen_name_value \
?creep_stress_value \
?matl_designation_value \
?img_analysis \
?img \
?calibr_factor_value \
?coord_x_value \
?coord_y_value \
?radius_nm_value

WHERE {
?tem_proc pmdco:input ?specimen .
?tem_proc a pmdco:TransmissionElectronMicroscopy .
?tem_proc pmdco:nextProcess ?img_analysis .

?specimen a pmdco:Specimen .
?specimen pmdco:characteristic ?matl_designation .
?specimen pmdco:characteristic ?creep_stress .
?specimen pmdco:characteristic ?specimen_name .
?matl_designation a pmdco:MaterialDesignation .
?matl_designation pmdco:value ?matl_designation_value .
?creep_stress a pmdco:CreepStress .
?creep_stress pmdco:value ?creep_stress_value .
?specimen_name a pmdco:SpecimenName .
?specimen_name pmdco:value ?specimen_name_value .

?img_analysis pmdco:input ?img .
?img_analysis pmdco:output ?coord_x .
?coord_x a pgo:WeightedXCoordinate .
?coord_x pmdco:value ?coord_x_value .
?img_analysis pmdco:output ?coord_y .
?coord_y a pgo:WeightedYCoordinate .
?coord_y pmdco:value ?coord_y_value .
?img_analysis pmdco:output ?radius .
?radius a pgo:ParticleRadius .
?radius pmdco:unit qudt:NanoM .
?radius pmdco:value ?radius_nm_value .

?img pmdco:characteristic ?calibr_factor .
?calibr_factor a pgo:CalibrationFactor .
?calibr_factor pmdco:unit pmdco:PixelPerNanometer .
?calibr_factor pmdco:value ?calibr_factor_value .
}

```

Box 1 SPARQL query to retrieve, e.g., the X and Y coordinates of precipitates.

Exploring Orowan strengthening through semantic data analysis. Building upon the semantic integration of the two distinct datasets outlined in Section [Implementation of RDF graphs and ABox data instantiation](#) and the newly obtained results from the Delaunay triangulation, we now apply these to explore the Orowan mechanism. The yield strength (σ_{ys}) of alloys can be modeled as the cumulative effect of various mechanisms:

$$\sigma_{ys} = \sigma_i + \sigma_{ss} + \sigma_p + \sigma_{gs} \quad (1)$$

Here, σ_i , σ_{ss} , σ_p , and σ_{gs} represent the intrinsic crystal, solid solution, precipitate strengthening, and grain size contributions, respectively. The precipitate strengthening component σ_p is typically expressed as the harmonic mean of contributions from dislocations shearing through shearable precipitates (particles) $\sigma_{Friedel}$ and bowing between non-shearable precipitates σ_{Orowan} . The contribution from dislocation bowing can in the idealized case be described as:

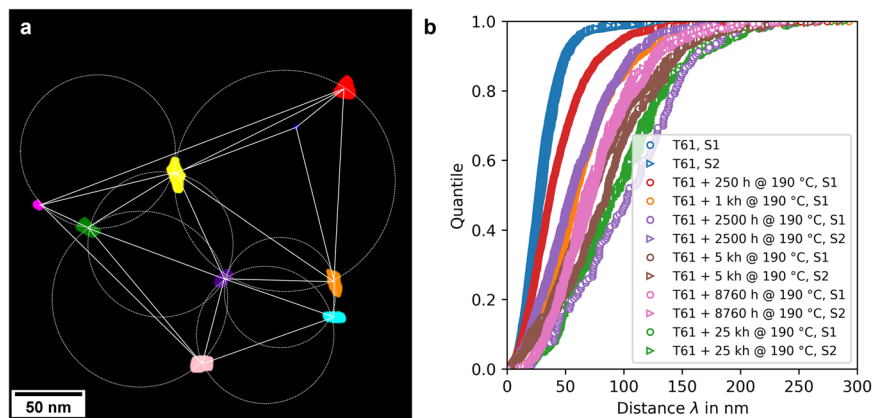


Fig. 1 Analysis of precipitate distances using Delaunay triangulation. **(a)** Application of Delaunay triangulation to a DF-TEM image from the T61 + 2,500 h @ 190 °C, S1 dataset, illustrating the measured distances between segmented precipitates. **(b)** Displayed as a cumulative distribution function plot, this illustrates the range of precipitate distances within different material states, with labels S1 and S2 denoting the specific samples examined (refer to Table 1).

$$\sigma_{\text{Orowan}} \propto \frac{G \cdot b}{\lambda} \quad (2)$$

In this equation, G , b , and λ are the shear modulus, the Burgers vector, and the edge-to-edge precipitate distance, respectively.

For our analysis, the material states exhibit significant variations primarily in the precipitate strengthening contribution σ_p , with other factors in Equation (1) remaining constant. By correlating DF-TEM observed precipitate distributions, characterized by λ_{mean} (represented by `pgo:AveragePrecipitateDistance` in the ontology), with tensile test-derived σ_{ys} values, we aim to illustrate the contribution of σ_{Orowan} to the overall yield strength. It should be noted, that the Orowan stress σ_{Orowan} is defined for a single dislocation while the yield strength determined on a tensile test piece $R_{p0.2}$ (represented by `tto:ProofStrengthPlasticExtension`) is the result of countless dislocation and an evaluation procedure prescribed by a standard. But it is common practice in materials science to correlate both.

Adhering to PMDco's fundamental concepts enables the formulation of a SPARQL query that aggregate properties like materials yield strength σ_{ys} and average precipitate distance λ into a unified dataset (see Box 2). This unified dataset can be represented in a tabular format or further processed for visualization, as shown in Figure 2.

Discussion

Establishing semantic interoperability. In this research, we have developed a demonstrator and described its functionality (Section Results and Section Implementation of RDF graphs and ABox data instantiation). The key components of this demonstrator are depicted in Figure 3. We employed an ontological framework that integrates the PMD Core Ontology (PMDco) with the Tensile Test Ontology (TTO) and the Precipitate Geometry Ontology (PGO) (Section Ontological framework). This setup enabled us to instantiate publicly available datasets from two different material characterization techniques sourced from Zenodo (see Data Availability statement).

The data from tensile testing and DF-TEM image analysis, while inherently different, have been transformed into interoperable RDF triples through the application of the PMDco, TTO and PGO. This transformation is facilitated by the interconnected concepts within the PMDco, which serve as bridges between the TTO and PGO entities. Consequently, a knowledge graph is established, allowing for SPARQL queries to retrieve instances across both TTO and PGO, filtered by material state (see Box 2). This demonstrates the principle of semantic interoperability and highlights the effectiveness of query filters in correlating diverse data sources.

Expanding upon this foundation, the creation of new classes and instances via SPARQL-driven data analysis systematically enriches our knowledge graph. This illustrates the scalable nature of our approach. However, in ontology-centric data management, any changes to the ontology structure must be managed carefully to avoid impacting its functionality. Developing a consistent mid-level ontology, aligned with a standard top-level ontology like the BFO³⁶, can significantly enhance the interoperability of semantic data, extending well beyond the domain of MSE.

Future perspectives in MSE knowledge representation. As already described in more detail in Section Introduction, the potential for ontology-based knowledge representation in MSE is substantial. Our research has established a sound basis for creating and expanding explicit knowledge representations in this field.

Looking ahead, the scope of MSE knowledge representation is expected to evolve beyond the current explicit modeling techniques. It will increasingly incorporate logical and computational methods to derive new insights and refine data curation practices. Central to this evolution is the role of reasoning. Our work has already

```

PREFIX pmdco: <https://w3id.org/pmd/co/>
PREFIX pgo: <https://w3id.org/pmd/pgo/>
PREFIX tto: <https://w3id.org/pmd/tto/>

SELECT DISTINCT ?matl_designation_tem_specimen \
                ?proc_TEM \
                ?mean_distance_value \
                ?mean_distance_unit \
                ?proc_TT \
                ?rp02_value \
                ?rp02_unit

WHERE {
# Match a specimen that has an pgo:AveragePrecipitateDistance as characteristic.
?mean_distance a pgo:AveragePrecipitateDistance .
?mean_distance pmdco:value ?mean_distance_value .
?mean_distance pmdco:unit ?mean_distance_unit .
?specimen pmdco:characteristic ?matl_designation_tem .
?specimen pmdco:characteristic ?mean_distance .
?matl_designation_tem a pmdco:MaterialDesignation .
?matl_designation_tem pmdco:value ?matl_designation_tem_specimen .

# Match a specimen that is input to a TEM-process and has a material designation.
?proc_TEM a pmdco:TransmissionElectronMicroscopy .
?proc_TEM pmdco:input ?specimen .
?specimen a pmdco:Specimen .

# Match a tensile test at 20 C that has Rp02 as output and a characteristic
# material designation.
?proc_TT a tto:TensileTest .
?proc_TT pmdco:characteristic ?test_tempr .
?test_tempr a pmdco:EnvironmentalTemperature .
?test_tempr pmdco:value "20"^^xsd:float .
?proc_TT pmdco:characteristic ?matl_designation_tt .
?matl_designation_tt a pmdco:MaterialDesignation .
?matl_designation_tt pmdco:value ?matl_designation_tt_specimen .
?proc_TT pmdco:output ?output .
?output a tto:Rp02 .
?output pmdco:value ?rp02_value .
?output pmdco:unit ?rp02_unit .

# Keep those whose material designation is equal
FILTER (str(?matl_designation_tem_specimen)=str(?matl_designation_tt_specimen))
}

```

Box 2 SPARQL query for retrieving the correlatable proof strength plastic extension and their mean precipitate distance values.

provided a glimpse into the potential of reasoning (see Figure 4). In this context, for instance, the object property was InfluencedBy denotes the inclusion of a specific and well-known strain rate in the dataset. As every process output is semantically connected to its inputs and characteristics, the ontology-based logic exposes the connection between yield stress (output of the process) and strain rate (characteristic of the process). This relationship is inherently semantic, which still has to be interpreted from a materials science perspective. As a result of our linked data processing in Protégé, the reasoning procedure successfully generated about 58,000 new triples. In general, reasoning, through the application of logical rules of ontologies, opens up new avenues for insight. Particularly intriguing is the automatic identification of inconsistencies, ensuring the relevance and accuracy of instantiated data. By integrating reasoning as a core method, we can develop more comprehensive and adaptable knowledge graphs, enhancing the MSE field's capacity to manage and interpret complex data relationships.

Additionally, the use of languages and tools such as the Semantic Web Rule Language (SWRL)³⁷ and Drools³⁸ will provide further possibilities for optimizing knowledge representations. SWRL, which integrates the Web Ontology Language (OWL) with the Rule Interchange Format (RIF), lays a solid basis for complex inference and deduction processes crucial for understanding MSE data in depth³⁹. This rule-based inference can significantly enhance the semantic richness of our approach. Furthermore, the integration of Drools as a rule engine marks a step forward in decision support and process automation, aligning with the specific data and contextual requirements of MSE.

Limitations and outlook. In ontology-based data management, the reliance on SPARQL for query activities is a notable challenge. SPARQL's complexity necessitates specific technical skills, posing a barrier to users unfamiliar with its syntax and the structure of RDF data^{40,41}. To enhance user accessibility, future tools should focus on natural language processing capabilities, fostering an environment where queries are based more on intuitive human communication.

Interoperability of workflows and the adaptability of ontologies to diverse datasets also present critical areas for development in MSE. Current approaches are often tailored to specific datasets and limit broader application. Future efforts should aim at developing ontologies that are both robust and flexible, capable of handling varied data types and evolving information. Enhancing workflow interoperability is essential for managing the

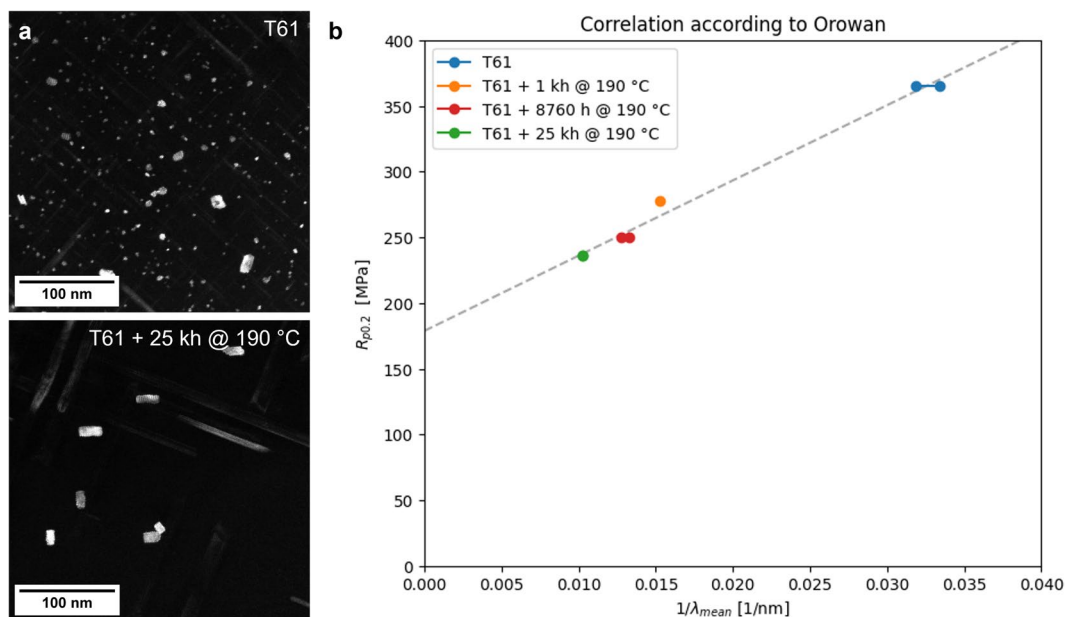


Fig. 2 Impact of aging on material properties. (a) Displays examples of DF-TEM images for different material states: the upper image shows the T61 initial state, and the lower image depicts the state after aging at 190 °C for 25,000 h. Notably, aging leads to coarsening, with precipitates becoming fewer and larger, thereby increasing the average precipitate distance. (b) Presents a plot derived from SPARQL query results, illustrating the dataset's alignment with the expected trend of $\sigma_{ys} \propto 1/\lambda$, as per Equation (2). It is important to note that tensile test data were available for only four material states, and the SPARQL query was employed to filter and identify six data point pairs for correlation across both mechanical and microstructural datasets.

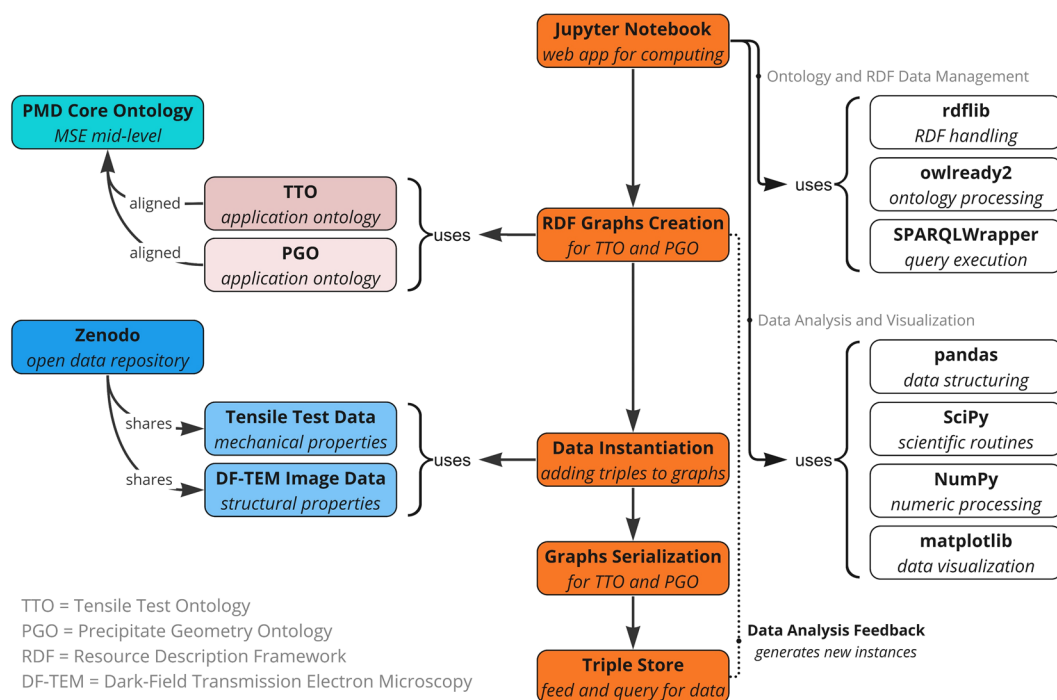


Fig. 3 Key components of the demonstrator. This diagram outlines the key components and workflow of an ontology-centric data analysis framework within MSE. It encompasses the creation of RDF graphs, ontology alignment, data serialization, interactions with the local triple store, and the utilization of various libraries within the Jupyter Notebook environment. Our framework also involves analytical and visualization libraries for data processing, with a feedback loop for continuous development, and data sharing through Zenodo.

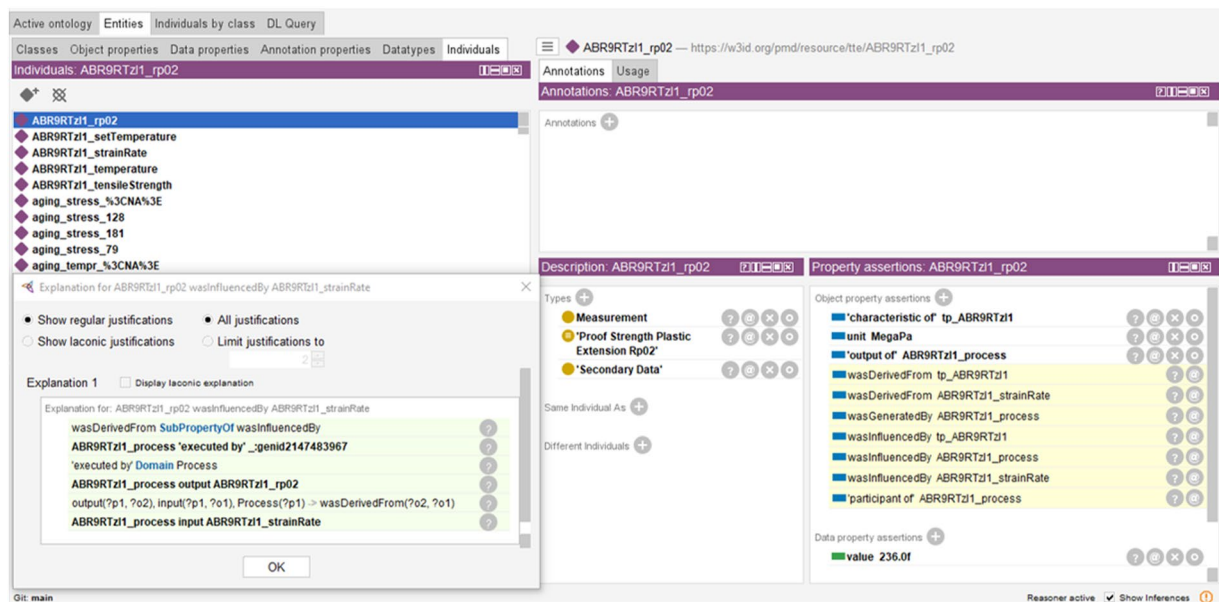


Fig. 4 Exploring implicit MSE knowledge through reasoning. This screenshot demonstrates the implicit knowledge discovered by reasoning with Pellet in Protégé. It illustrates, for example, the inferred semantic connection between yield stress (the output of the process) and strain rate (a characteristic of the process) as applied in the experimental setup.

increasing volumes of data efficiently, thereby unlocking the full potential of semantic technologies in MSE for multidisciplinary research and insights.

Summary. As a key outcome of our work, a demonstrator is provided that facilitates the interoperable linking of two publicly available datasets. These datasets, derived from distinct mechanical and structural characterization techniques of an aluminum alloy, are cohesively integrated using ontologies. The utilization of the PMDCo enhances data usability and exemplifies practical effectiveness of semantic interoperability.

We have demonstrated the ability to query the constructed knowledge graph for specific information using SPARQL queries. This capability of generating new data from these queries, which then enriches the knowledge graph, underscores the dynamic and evolving nature of knowledge graphs. The continuous enrichment and expansion of the graph are key features of our approach.

Our work serves as a systematic and reproducible example of how data management and analysis in MSE can be aligned with FAIR principles, paving the way for future advancements. We also highlight key building blocks for semantic interoperability and create a basis which can be adapted and extended for different MSE applications.

In addition, our approach has shown the potential of Semantic Web technologies in uncovering hidden patterns across distinct datasets, making them potentially accessible and interpretable by machines. This opens new avenues for in-depth data analysis and insight generation, with machines playing a pivotal role in identifying trends and relationships that may not be immediately apparent to human researchers.

In summary, our study makes an important contribution to the field of MSE by providing tools and methods for semantic data integration, management, and analysis. These advancements enhance the field's capacity to leverage data for advanced research and applications, marking a notable step forward in data-driven materials science exploration.

Methods

Sample material and states. Our study builds upon the prior research by Rockenhäuser *et al.*^{34,42}, which focused on the coarsening processes of the S-phase in the aluminum alloy EN AW-2618A under elevated temperature conditions. In their experiments, the specimens underwent aging at 190 °C, extending up to 25,000 h. This process was followed by a detailed characterization of the evolved microstructure. The specimens were initially prepared in the T61 condition, a procedure that included solution annealing at 530 °C for 8 h, followed by rapid quenching in boiling water. Subsequent aging was conducted at 195 °C for a period of 28 h.

Tensile testing. The tensile test dataset, accessible on Zenodo³¹, was compiled from tensile tests performed in accordance with the ISO 6892-1 standard⁴³. These tests were conducted at a constant strain rate of 10^{-4} 1/s, utilizing B6 x 30 tensile test specimens, as specified by DIN 50125⁴⁴.

DF-TEM imaging. In our work, we utilized an image analysis dataset (see Table 1) from the aforementioned previous investigation by Rockenhäuser *et al.*, accessible on Zenodo³². The dataset includes analysis data of dark-field transmission electron microscopy (DF-TEM) images focusing on S-phase precipitates within the

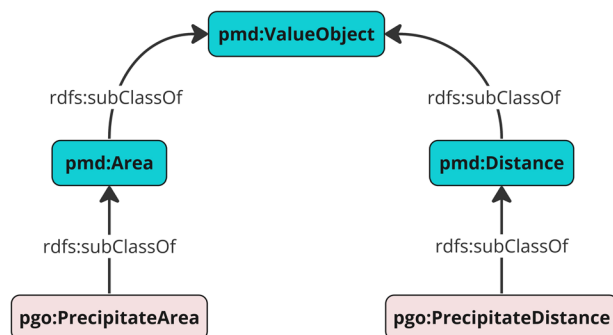


Fig. 5 Class hierarchy in the Precipitate Geometry Ontology (PGO). This figure illustrates PGO's application-specific subclasses, such as `pgo:PrecipitateArea` and `pgo:PrecipitateDistance`, extending from PMDCo's general `pmdco:ValueObject` class via `pmdco:Area` and `pmdco:Distance`, respectively.

aluminum matrix. The original DF-TEM images were captured with a JEM-2200FS TEM, operating at 200 kV, with specimens aligned along the [001] crystallographic direction. The DF-TEM images were provided in the dm3 format, a 16-bit raster format specifically designed for electron microscopy. This format includes vital meta-data about the TEM procedure, such as details on the CCD camera, exposure time, and more.

To facilitate analysis, primarily the rod axis of the rod-shaped S-phase precipitates perpendicular to the image plane was imaged (The S-phase precipitates appear bright against a dark background). In addition, the precipitates were assumed to be cylindrical. The image-based evaluation was conducted on processed DF-TEM images using ImageJ software⁴⁵. This process began with edge-preserving median filtering of the raw images, followed by manual thresholding for binarization. Such procedures enabled the exclusion of microstructural artifacts and horizontal rod-shaped precipitates from the analysis. The binarized image data facilitated the differentiation of the precipitates from the background. The dataset covers extensive evaluations of these images, with at least 300 precipitates analyzed for each material state. For an in-depth understanding of the materials, methodologies, and the software-based image analysis that yielded critical precipitate parameters like count, coordinates, area, and radius, readers are referred to the publications by Rockenhäuser *et al.*^{34,42}.

Software tools and libraries. The scripts for this work were developed within a Jupyter Notebook environment⁴⁶. We utilized various Python⁴⁷-based libraries, including:

- The `rdflib`⁴⁸ and `Owlready2`⁴⁹ packages, crucial for semantic data processing and graph-based representations, facilitating semantic data integration.
- `SPARQLWrapper` for simplifying remote SPARQL query execution and results conversion⁵⁰.
- `NumPy`⁵¹ and `pandas`⁵² for numerical operations.
- `matplotlib` for data visualizations⁵³.
- `SciPy` for advanced data manipulation and visualization tasks, including Delaunay triangulation⁵⁴.
- The Protégé ontology editor⁵⁵, supporting OWL 2 Web Ontology Language⁵⁶, for ontology design and Pellet for reasoning⁵⁷.

Ontologies and GitHub integration. The PMDCo Core Ontology (PMDco), Version 2.0.7, serves as the upper-level ontology, providing bridging mid-level concepts crucial for achieving semantic interoperability^{29,58}.

For the representation of tensile tests of metals at room temperature, aligned with ISO 6892-1:2019-11⁴³, we employed the Tensile Test Ontology (TTO)^{59,60}.

The Precipitate Geometry Ontology (PGO)⁶¹ is used for representing microstructural data derived from DF-TEM image analysis.

QUDT entities were incorporated for units of measure⁶².

GitHub is used for publishing, maintaining, and developing these ontologies along the associated scripts⁶³.

Ontological framework. This work utilizes an ontological framework structured around PMDCo, a mid-level ontology specifically developed for MSE. PMDCo is a foundational reference for semantically bridging more specialized MSE application ontologies, namely in our work, the TTO and the PGO. The TTO facilitates the systematic representation of tensile test data, while the PGO enables representation of microstructural data. Together these interconnected ontologies establish a semantic network that standardizes the representation, querying, and analysis of distinct datasets.

Achieving semantic interoperability with the PMDCo. The PMDCo plays a pivotal role in semantically inter-linking the TTO and the PGO. While each application ontology addresses specific domain-related classes, the PMDCo offers broader MSE concepts, ensuring the application ontologies are embedded in a structured,

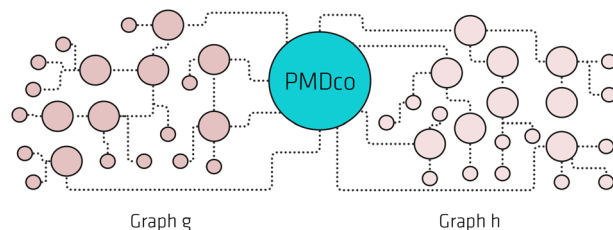


Fig. 6 Facilitating semantic integration via the PMDco. This diagram schematically depicts the semantic connections between two application ontologies, graphs “g” and “h”. The PMDco is a mid-level ontology, providing general MSE concepts crucial for bridging these ontologies.

extendable system. This framework allows for the addition of application-specific classes, crucial for representing diverse data sources coherently, thereby enhancing semantic interoperability.

Standardizing tensile test data with the TTO. Based on the PMDco, the Tensile Test Ontology (TTO) was designed to provide a structured vocabulary for tensile test data. Thereby, the test standard-compliant ontological representation ensures this data to be interoperable, transparent, reliable, and reproducible. Hence, the TTO is crucial in the semantic integration of tensile test data, particularly in this work concerning radial compressor wheel samples. Aligned with ISO 6892-1:2019-1 standard for tensile testing of metals at room temperature (see Section [Ontologies and GitHub integration](#)), the terminological box (TBox) of the TTO ensures a standardized approach for data integration. Therein, a comprehensive number of classes is included to specifically annotate data on characteristic values obtained from a tensile test, such as, e.g., yield strength (R_m), proof strength, plastic extension (R_p), and strain rate $\dot{\epsilon}_{L_e}$. Furthermore, semantic relationships are also implemented that enable logical reasoning and thus, lead to improved data interpretation capabilities (see Section [Future perspectives in MSE knowledge representation](#)). Overall, the TTO harmonizes tensile test data, which often varies in structure and format, into uniform RDF triples, thus improving data comparability and method reproducibility by incorporating essential contextual information, such as metadata and provenance⁵⁹.

Integrating microstructural data with the PGO. Integration of microstructural data from DF-TEM image analysis is accomplished using the Precipitate Geometry Ontology (PGO). Designed to extend PMDco’s class structure, the PGO introduces specific subclasses for a more detailed representation of precipitate data. These subclasses, such as `pgo:PrecipitateArea` and `pgo:PrecipitateDistance`, enhance the granularity of the data representation, facilitating the construction of an informative KG. Figure 5 illustrates an exemplary subclass hierarchy of the PGO in relation to the broader PMDco structure.

Implementation of RDF graphs and ABox data instantiation. In a Jupyter Notebook environment, we initiate the process by importing ontologies (i), constructing RDF graphs (ii), and instantiating ABox (Assertion Box) data (iii). These steps are supported by specific Python libraries, as detailed in Section [Software tools and libraries](#).

- (i) Initially, the PMDco and the application ontologies, including the TTO and PGO TBoxes, in Turtle format (ttl), are imported into the Notebook environment.
- (ii) We then proceed to construct distinct RDF graphs for integrating the datasets: “g” for tensile test data and “h” for DF-TEM image analysis data. Both graphs are aligned with the PMDco, providing an ontological framework for semantic interoperability (see Figure 6). Graph “g” encompasses tensile test entities such as measurement values, as well as the initial test pieces (input) and the resulting fractured halves (output) (see Figure 7(a)). It comprehensively details mechanical properties like yield and proof strength, environmental conditions during testing, and descriptions of the material states. Graph “h” focuses on microstructural data, representing precipitate characteristics such as the coordinates, areas, and distances. The RDF representations bridge mechanical and microstructural data, enabling flexible correlations within a unified semantic network.
- (iii) Subsequently, the tensile test and DF-TEM datasets are instantiated within these graphs. ABox instances are created based on the TBox classes and properties, utilizing RDF triples (subject, predicate, object) for data serialization. This process establishes the relationships between entities, with each assigned a unique Internationalized Resource Identifier (IRI) for identification (refer to Figure 7), thereby enabling advanced data querying and analysis⁶⁴.

Data availability

The tensile test dataset³¹ and the TEM microstructural analysis dataset³², both hosted on Zenodo, are integral to our study. The tensile test dataset delivers comprehensive results from tests conducted on EN AW-2618A aluminium alloy. The TEM dataset provides detailed quantitative analysis of the microstructure of the same alloy, with a particular emphasis on examining the S-phase Al_2CuMg parameters. The RDF graph data, resulting from

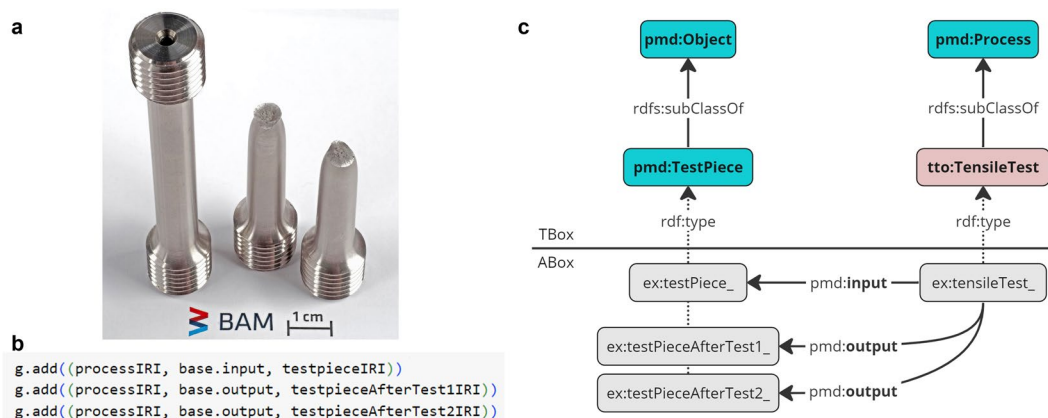


Fig. 7 Tensile test pieces and RDF integration. (a) Tensile test pieces before and after testing, showing intact and fractured states. (b) RDF triple integration in tensile testing, illustrated by `g.add((processIRI, base.input, testpieceIRI))`. In this context, the tensile test piece (denoted by `testpieceIRI`) is the input (identified by `base.input`) and output (identified by `base.output`) for the tensile test process (represented by `processIRI`). (c) Schematic of PMDco's role in connecting TTO entities in tensile testing. Instances such as `ex:testPiece_`, `ex:testPieceAfterTest1_`, and `ex:testPieceAfterTest2_` are categorized under `pmd:TestPiece` class using the `rdf:type` property.

the semantic integration of these two datasets, is available on GitHub. Access to the Tensile test RDF graph data, the DF-TEM RDF graph data, the DF-TEM RDF graph data addition, and the demo-orowan RDF graph:

- [Tensile test RDF graph data](#)
- [DF-TEM RDF graph data](#)
- [DF-TEM RDF graph data addition](#)
- [demo-orowan RDF graph data](#)

Code availability

The script and the ontologies utilized in this study are openly accessible and can be obtained from the following GitHub repositories:

- [demo-orowan](#)
- [PMD Core Ontology \(PMDco\)](#)
- [Tensile Test Ontology \(TTO\)](#)
- [Precipitate Geometry Ontology \(PGO\)](#)

Received: 15 January 2024; Accepted: 20 March 2024;

Published online: 30 April 2024

References

1. Kalidindi, S. R. & Graef, M. D. Materials data science: Current status and future outlook. *Annual Review of Materials Research* **45**, 171–193 (2015).
2. Kimmig, J., Zechel, S. & Schubert, U. S. Digital transformation in materials science: A paradigm change in material's development. *Advanced Materials* **33**, 2004940 (2021).
3. Ward, C. H., Warren, J. A. & Hanisch, R. J. Making materials science and engineering data more valuable research products. *Integrating Materials and Manufacturing Innovation* **3**, 292–308 (2014).
4. Prakash, A. & Sandfeld, S. Chances and challenges in fusing data science with materials science. *Practical Metallography* **55**, 493–514 (2018).
5. Mrdjenovich, D. *et al.* propnet: A knowledge graph for materials science. *Matter* **2**, 464–480 (2020).
6. Hippalgaonkar, K. *et al.* Knowledge-integrated machine learning for materials: Lessons from gameplaying and robotics. *Nature Reviews Materials* **8**, 241–260 (2023).
7. Wilkinson, M., Dumontier, M. & Aalbersberg, I. *et al.* The FAIR guiding principles for scientific data management and stewardship. *Scientific Data* **3**, 160018 (2016).
8. Hawke, S., Herman, I., Archer, P. & Prud'hommeaux, E. W3C Semantic Web. <https://www.w3.org/2001/sw/> Accessed: 2024-01-09 (2013).
9. Valdestilhas, A., Bayerlein, B., Moreno Torres, B., Ghezal Ahmad, J. Z. & Muth, T. The intersection between Semantic Web and materials science. *Advanced Intelligent Systems* **5**, 2300051 (2023).
10. Zhang, X., Zhao, C. & Wang, X. A survey on knowledge representation in materials science and engineering: An ontological perspective. *Computers in Industry* **73**, 8–22 (2015).
11. Domingue, J., Fensel, D. & Hendler, J. A. (eds) *Handbook of Semantic Web Technologies* (Springer, Berlin, Heidelberg, 2011).
12. Gruber, T. R. A translation approach to portable ontology specifications. *Knowledge Acquisition* **5**, 199–220 (1993).
13. Brewster, C. & O'Hara, K. Knowledge representation with ontologies: Present challenges – Future possibilities. *International Journal of Human-Computer Studies* **65**, 563–568 (2007).

14. Broeckmann, C. *et al.* Materials Within a Digitalized Production Environment, 1–15 (Springer International Publishing, Cham, 2023).
15. Noy, N., McGuinness, D. L. & Lierler, Y. Research challenges and opportunities in knowledge representation. (eds Noy, N. & McGuinness, D. L.) *Final Report on the 2013 NSF Workshop on Research Challenges and Opportunities in Knowledge Representation*. <https://corescholar.libraries.wright.edu/cgi/viewcontent.cgi?article=1217&context=cse> (2013).
16. Ghiringhelli, L. M. *et al.* Shared metadata for data-centric materials science. *Scientific Data* **10**, 626 (2023).
17. Guarino, N., Oberle, D. & Staab, S. *What Is an Ontology?* 1–17 (Springer, Berlin, Heidelberg, 2009).
18. Rudnicki, R., Smith, B., Malyuta, T. & Mandrick, W. Best practices of ontology development. https://www.nist.gov/system/files/documents/2021/10/14/nist-ai-rfi-cubrc_inc_002.pdf. White Paper (2013).
19. RDF Working Group. Resource Description Framework (RDF). <https://www.w3.org/RDF/> Accessed: 2024-01-09 (2014)
20. Takahashi, L. & Takahashi, K. Visualizing scientists' cognitive representation of materials data through the application of ontology. *The Journal of Physical Chemistry Letters* **10**, 7482–7491 (2019).
21. Bayerlein, B. *et al.* A perspective on digital knowledge representation in materials science and engineering. *Advanced Engineering Materials* **24**, 2101176 (2022).
22. Gupta, T., Zaki, M., Krishnan, N. M. & Mausam, A. Matscibert: A materials domain language model for text mining and information extraction. *npj Computational Materials* **8**, 102 (2022).
23. Sequeda, J., Allemang, D. & Jacob, B. A benchmark to understand the role of knowledge graphs on large language model's accuracy for question answering on enterprise SQL databases (2023).
24. Bock, F. E. *et al.* A review of the application of machine learning and data mining approaches in continuum materials mechanics. *Frontiers in Materials* **6**, 1–23 (2019).
25. Schmidt, J., Marques, M. R. G., Botti, S. & Marques, M. A. L. Recent advances and applications of machine learning in solid-state materials science. *npj Computational Materials* **5**, 1–36 (2019).
26. Liu, J. & Qian, Q. Reinforcement learning-based knowledge graph reasoning for aluminum alloy applications. *Computational Materials Science* **221**, 112075 (2023).
27. Himanen, L., Geurts, A., Foster, A. S. & Rinke, P. Data-driven materials science: Status, challenges, and perspectives. *Advanced Science* **6**, 1900808 (2019).
28. Gottstein, G. *Physikalische Grundlagen der Materialkunde*, Ch. 6.7 Mechanismen der Festigkeitssteigerung, 259 – 264 (Springer, Berlin, Heidelberg, 2007).
29. Bayerlein, B. *et al.* PMD Core Ontology: Achieving semantic interoperability in materials science. *Materials & Design* **237**, 112603 (2024).
30. Bayerlein, B., Schilling, M., v. Hartrott, P. & Waitelonis, J. demo-orowan. <https://github.com/materialdigital/demo-orowan> Accessed: 2024-01-09 (2023).
31. von Hartrott, P. & Skrotzki, B. Room temperature and elevated temperature tensile test and elastic properties data of Al-alloy EN AW-2618A after different aging times and temperatures. *Zenodo* <https://doi.org/10.5281/zenodo.10377164> (2023).
32. Rockenhäuser, C. & Skrotzki, B. Radii of S-phase Al₂CuMg in Al-alloy EN AW-2618A after different aging times at 190 °C. *Zenodo* <https://doi.org/10.5281/zenodo.7625259> (2023).
33. Harris, S., Seaborne, A. & Prud'hommeaux, E. SPARQL 1.1 query language. <https://www.w3.org/TR/sparql11-query/> Accessed: 2024-01-09 (2013).
34. Rockenhäuser, C., Schrieber, S., Hartrott, P., Piesker, B. & Skrotzki, B. Comparison of long-term radii evolution of the S-phase in aluminum alloy 2618A during ageing and creep. *Materials Science and Engineering: A* **716**, 78–86 (2018).
35. Delaunay, B. *et al.* Sur la sphère vide. *Izv. Akad. Nauk SSSR, Otdelenie Matematicheskii i Estestvennyka Nauk* **7**, 1–2 (1934).
36. International Organisation for Standardisation. Information technology - Top-level ontologies (TLO) - part 2: Basic Formal Ontology (BFO) (ISO/IEC 21838-2:2021(E)). <https://www.beuth.de/de/norm/iso-iec-21838-2/348948268> (2021).
37. Horrocks, I. *et al.* SWRL: A Semantic Web Rule Language combining OWL and RuleML. <https://www.w3.org/submissions/SWRL/> Accessed: 2024-01-09 (2004).
38. Proctor, M. Schürr, A., Varró, D. & Varró, G. (eds) Drools: A rule engine for complex event processing. (eds Schürr, A., Varró, D. & Varró, G.) *Applications of Graph Transformations with Industrial Relevance*, 2–2 (Springer, Berlin, Heidelberg, 2012).
39. RIF Working Group. RIF FAQ. https://www.w3.org/2005/rules/wiki/RIF_FAQ Accessed: 2024-01-09 (2013).
40. Ngonga Ngomo, A.-C., Bühmann, L., Unger, C., Lehmann, J. & Gerber, D. for Computing Machinery, A. (ed.) *Sorry, I don't speak SPARQL: Translating SPARQL queries into natural language*. (ed. for Computing Machinery, A.) *Proceedings of the 22nd International Conference on World Wide Web, WWW '13*, 977–988 (Association for Computing Machinery, New York, NY, USA, 2013).
41. Ochieng, P. PAROT: Translating natural language to SPARQL. *Expert Systems with Applications: X* **5**, 100024 (2020).
42. Rockenhäuser, C. *et al.* On the long-term aging of S-phase in aluminum alloy 2618A. *Journal of Materials Science* **56**, 8704–8716 (2021).
43. International Organisation for Standardisation. Metallic materials - tensile testing - part 1: Method of test at room temperature (EN ISO 6892-1:2016). <https://www.beuth.de/de/norm/din-en-iso-6892-1/244454003> (2017).
44. International Organisation for Standardisation. Testing of metallic materials - tensile test pieces (DIN 50125:2016-12) (2016).
45. Schneider, C., Rasband, W. & Eliceiri, K. NIH Image to ImageJ: 25 years of image analysis. *Nature Methods* **p**, 671–675 (2012).
46. Kluyver, T. *et al.* Jupyter Notebooks - A publishing format for reproducible computational workflows (IOS Press, Amsterdam, 2016).
47. Van Rossum, G. & Drake, F. L. Python 3 Reference Manual (CreateSpace, Scotts Valley, CA, 2009).
48. Boettiger, C. rdflib: A high level wrapper around the redland package for common RDF applications. *Zenodo* (2018).
49. Lamy, J.-B. Owlready: Ontology-oriented programming in Python with automatic classification and high level constructs for biomedical ontologies. *Artificial Intelligence in Medicine* **80**, 11–28 (2017).
50. RDFLib Contributors. SPARQL endpoint interface to Python. <https://rdflib.dev/sparqlwrapper/doc/1.8.5/main.html> Accessed: 2024-01-09 (2020).
51. Harris, C. R. *et al.* Array programming with NumPy. *Nature* **585**, 357–362 (2020).
52. The Pandas development team. pandas-dev/pandas: Pandas (2020).
53. Hunter, J. D. Matplotlib: A 2D graphics environment. *Computing in Science & Engineering* **9**, 90–95 (2007).
54. Virtanen, P. *et al.* SciPy 1.0: Fundamental Algorithms for Scientific Computing in Python. *Nature Methods* **17**, 261–272 (2020).
55. Knublauch, H., Ferguson, R. W., Noy, N. & Musen, M. A. Goos, G. & Hartmanis, J. (eds) The Protégé OWL plugin: An open development environment for Semantic Web applications. (eds Goos, G. & Hartmanis, J.) *International Workshop on the Semantic Web*. <https://api.semanticscholar.org/CorpusID:5705390> (2004).
56. Motik, B. *et al.* OWL 2 web ontology language: Structural specification and functional-style syntax. Tech. Rep., W3C. <http://www.w3.org/2007/OWL/draft/owl2-syntax/> (2008).
57. Sirin, E., Parsia, B., Grau, B. C., Kalyanpur, A. & Katz, Y. Pellet: A practical OWL-DL reasoner. *Journal of Web Semantics* **5**, 51–53 (2007).
58. Bayerlein, B. *et al.* PMDco: Platform Material Digital Core Ontology. version 2.0.7. <https://materialdigital.github.io/core-ontology/> Accessed: 2024-01-09 (2023).
59. Schilling, M. *et al.* FAIR and structured data: A standard-compliant domain ontology for tensile testing. *Advanced Engineering Materials* **2400138**, 1–19 (2024).

60. Schilling, M., Bayerlein, B., Birkholz, H., v. Hartrott, P. & Waitelonis, J. TTO: Tensile Test Ontology. version 2.0.1. <https://materialdigital.github.io/application-ontologies/tto/> Accessed: 2024-01-09 (2023).
61. Schilling, M. & Bayerlein, B. PGO: Precipitate Geometry Ontology. version 1.0.0. <https://materialdigital.github.io/application-ontologies/pgo/> Accessed: 2024-01-09 (2023).
62. FAIRsharing. QUDT; quantities, units, dimensions and types. Accessed: 2024-01-09 (2022).
63. github. GitHub. <https://github.com/> Accessed: 2024-01-09 (2008).
64. Network Working Group. Internationalized Resource Identifiers (IRIs). <https://www.ietf.org/rfc/rfc3987> Accessed: 2024-01-09 (2005).

Acknowledgements

The authors thank the German Federal Ministry of Education and Research (BMBF) for financial support of the project **Innovation-Platform MaterialDigital** through project funding FKZ no: 13XP5094E (BAM), 13XP5094B (IWM), and 13XP5094F (FIZ). Moreover the authors would also like to thank Pedro D. Portella for all the valuable discussions on this topic. Thanks also to Dirk Bettge for the tensile test piece image.

Author contributions

B.B. drafted and wrote the original manuscript, and created the visualizations. He played an important role in the development and the implementation of the ontologies. M.S. was instrumental in the design of the ontologies and their technical implementation. P.v.H. participated in the manuscript preparation, was significantly involved in scripting and contributed to the design of the ontologies. J.W. supervised the technical aspects of the implementation of ontologies and script. All authors were actively involved in the conceptualization of the research and made essential contributions to the review and revision of the manuscript.

Funding

Open Access funding enabled and organized by Projekt DEAL.

Competing interests

The authors declare no competing interests.

Additional information

Correspondence and requests for materials should be addressed to B.B.

Reprints and permissions information is available at www.nature.com/reprints.

Publisher's note Springer Nature remains neutral with regard to jurisdictional claims in published maps and institutional affiliations.



Open Access This article is licensed under a Creative Commons Attribution 4.0 International License, which permits use, sharing, adaptation, distribution and reproduction in any medium or format, as long as you give appropriate credit to the original author(s) and the source, provide a link to the Creative Commons licence, and indicate if changes were made. The images or other third party material in this article are included in the article's Creative Commons licence, unless indicated otherwise in a credit line to the material. If material is not included in the article's Creative Commons licence and your intended use is not permitted by statutory regulation or exceeds the permitted use, you will need to obtain permission directly from the copyright holder. To view a copy of this licence, visit <http://creativecommons.org/licenses/by/4.0/>.

© The Author(s) 2024